JACS
JOURNAL OF THE AMERICAN CHEMICAL SOCIETY

Communication

pubs.acs.org/JACS

Tau Binds to Multiple Tubulin Dimers with Helical Structure

Xiao-Han Li,[†] Jacob A. Culver,[‡] and Elizabeth Rhoades*[,§,∥]

[†]Department of Chemistry, Yale University, New Haven, Connecticut 06520, United States

[‡]Ball State University, Muncie, Indiana 47306, United States

[§]Department of Molecular Biophysics and Biochemistry and Department of Physics, Yale University, New Haven, Connecticut 06520, United States

Supporting Information

ABSTRACT: Understanding the mechanism by which tau binds to and promotes microtubule (MT) assembly as part of its native function may also provide insight into its loss of function that occurs in neurodegenerative disease. Both mechanistic and structural studies of tau have been hindered by its intrinsic disorder and highly dynamic nature. Here, we combine fluorescence correlation spectroscopy and acrylodan fluorescence screening to study the stoichiometry and structural features of tau-tubulin assemblies. Our results show that tau binds to multiple tubulin dimers, even when MT assembly is inhibited. Moreover, we observe helical structure in the repeat regions of the MT binding domain of tau in the tau-tubulin complex, reflecting partial folding upon binding. Our findings support a role for tau's intrinsic disorder in providing a flexible scaffold for binding tubulin and MTs and a disorder-to-order transition in mediating this important interaction.

Tau is a microtubule (MT)-associated protein (MAP) which stabilizes MTs and promotes their assembly.[1] It is normally found distributed along the axons of neuronal cells, where it functions both in the establishment of cell polarity[2] and in the maintenance of axons.[3] Tau is further thought to play an important role in axonal transport,[4] and it has been reported to alter the activity of several MT motor proteins.[5] In Alzheimer's disease and other tauopathies, tau forms aggregated intracellular deposits; its loss of function plays an important role in pathology.[4,6]

Tau consists of a MT binding region (MTBR) composed of imperfect repeats[7] (R1, R2, R3, and R4), flanked by a proline-rich region (P1 and P2) that enhances MT binding and assembly,[8] and an N-terminal projection domain with putative roles in MT spacing[9] and membrane anchoring[10] (Figure 1). Each repeat consists of an inter-repeat or linker region and the conserved sequence (Figure 1). Initial biochemical studies depicted the repeat regions as binding weakly to MTs with the inter-repeats acting as spacers between them.[7] More recently it has been shown that the inter-repeats are also directly involved in MT binding and polymerization,[11] with the proline-rich region playing a regulatory role.[12]

Tau belongs to the class of intrinsically disordered proteins, so-called because of their lack of stable secondary structure and tertiary contacts under physiological solution conditions.

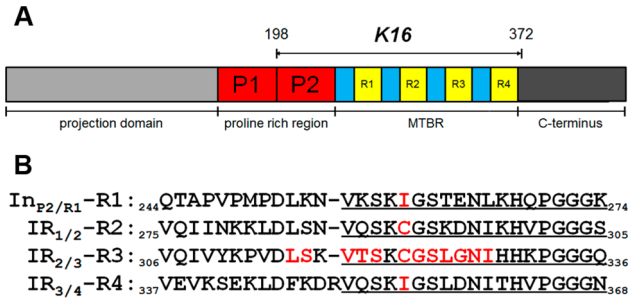

Figure 1. Schematic and sequence of tau. (A) The longest isoform of tau 2N4R illustrating major domains, with the proline-rich regions (P1, P2) and microtubule binding repeats (R1, R2, R3, R4), important for binding tubulin and microtubules colored explicitly. The K16 construct (residues 198−372) used in this study is indicated on the schematic. (B) The sequence of the microtubule binding region (numbering from 2N4R) with the consensus sequences of each repeat underlined and the positions labeled with acrylodan highlighted in red.

Because of its importance to maintaining functional MTs, there have been extensive efforts to resolve the structure of tau bound to MTs. Cryo-EM images suggest that tau becomes partially structured upon binding, although structural features were not resolved.[13] Both nascent α-helical and β-sheet structure in regions thought to be important for MT binding have been observed in solution by NMR.[14] More recently, our laboratory used single-molecule FRET to demonstrate that the MTBR is extended when bound to soluble tubulin.[15]

Despite the fact that tau has been heavily studied for almost 40 years, there are still many questions regarding its interaction with tubulin and MTs and its mechanism of function. In the study presented here, we use a combination of fluorescence correlation spectroscopy (FCS) and acrylodan fluorescence screening to elucidate structural details of tau bound to soluble tubulin. We find that tau is capable of binding to multiple tubulin dimers without causing assembly into MTs. Moreover, the repeat regions bind differentially and with apparent helical structure. This work offers the most explicit evidence of secondary structure in the MTBR of tau upon binding to tubulin to date. Moreover, it provides insight into a potential mechanism for tau-mediated polymerization of tubulin.

The interaction between tau and soluble tubulin was probed using fluorescence correlation spectroscopy (FCS). In FCS, the

Received: May 7, 2015
Published: July 12, 2015

DOI: 10.1021/jacs.5b04561
J. Am. Chem. Soc. 2015, 137, 9218−9221

temporal autocorrelation of spontaneous fluctuations in fluorescence intensity is fit with a suitable model to yield quantitative parameters associated with diffusion, concentration, and kinetics.[16] Here, we used FCS to analyze diffusion, which is dependent upon the size of the fluorescent molecules. The binding of fluorescently labeled tau to unlabeled tubulin results in a shift in the autocorrelation curve to longer decay times (Figure 2A), reflecting the slower diffusion of the

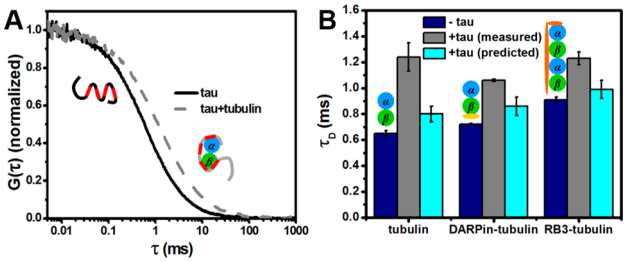

Figure 2. Characterization of tau-tubulin complex by FCS. (A) Normalized autocorrelation curves for fluorescently labeled tau in the absence (black solid) or presence (gray dashed) of 15 μM unlabeled tubulin. The curve shifts to the right, reflecting the larger τ_D of the tau-tubulin complex. Inset cartoon illustrates the change in size of fluorescent species. (B) τ_Ds of protein-tubulin complexes in the absence (navy) or presence (gray) of tau. In the absence of tau, measurements were made using fluorescently labeled tubulin, DARPin, or RB3, respectively; in the presence of tau, fluorescently labeled tau was used. Predicted τ_Ds for these complexes assuming that tau binds with 1:1 stoichiometry to tubulin, DARPin-tubulin, or RB3-tubulin (cyan). Cartoons of tubulin dimer (blue/green) with DARPin (yellow) or RB3 (orange) are based on crystal structures. The error bar indicates plus or minus one standard deviation for the experimental values, and the data range for predicted values.

complex. These measurements were performed under non-assembly conditions (20 °C, no GTP), with the concentration of tau low enough (~20 nM) to inhibit tau-promoted polymerization of tubulin. The autocorrelation curves were fit to a model with a single diffusing fluorescent species (see Supporting Information (SI)) to extract the average diffusion times, τ_D, of 0.60 ± 0.02 ms for tau and 1.24 ± 0.11 ms for the tau-tubulin complex (Figure 2B). Fluorescently labeled tubulin was measured separately to obtain an independent assessment of its diffusion time (τ_D = 0.65 ± 0.02 ms) (Figure 2B; SI, Table S1 for control measurements of all proteins).

Two proteins engineered to inhibit tubulin polymerization were used to further probe the tau-tubulin complex. Designed Ankyrin Repeat Protein (DARPin) binds to a single tubulin heterodimer in a 1:1 stoichiometry to form a β-capped DARPin-tubulin complex,[17] while Stathmin-like RB3 domain (RB3) binds to tubulin with a 1:2 stoichiometry to form a longitudinal dimer of tubulin dimers[18] (Figure 2B, cartoons). For FCS measurements, DARPin and RB3 were fluorescently labeled and incubated with excess unlabeled tubulin. As expected, DARPin-tubulin (τ_D = 0.72 ± 0.01 ms) diffuses more slowly than tubulin alone, but more rapidly than RB3-tubulin (τ_D = 0.91 ± 0.02 ms) (Figure 2B). Importantly, both complexes have faster diffusion times than tau-tubulin (Figure 2B). Comparison of the three tubulin complexes reveals that tau-tubulin has a significantly larger hydrodynamic radius compared with the two complexes with known structures. Interestingly, when fluorescent tau is added to unlabeled DARPin-tubulin or RB3-tubulin complexes, the diffusion times increase to τ_D = 1.06 ± 0.01 ms and τ_D = 1.23 ± 0.05 ms, respectively (Figure 2B).

In order to gain more insight into the molecular size of the tau-tubulin complex, models of tau were created by random sampling of dihedral angles from a Ramachandran plot and then adjusted to match our previously reported smFRET value for one pairwise distance across the MTBR.[15] These models were docked to tubulin, DARPin-tubulin, or RB3-tubulin using ZDOCK[19] with a 1:1 stoichiometry between tau and each complex. The top ten hits in each entry were used to calculate predicted diffusion times for comparison with experiments (Figure 2B; see SI for details). For all three complexes, the predicted diffusion times are significantly smaller than our measured values (Figure 2B, compare cyan and gray bars). These data demonstrate that the tau-tubulin complexes consist of a single tau bound to multiple tubulin dimers, even in the presence of proteins which block MT assembly.

While the FCS measurements allow for the assessment of bulk features of the tau-tubulin complex, they do not provide information about possible secondary structure of tau upon binding. To investigate this, tau was labeled throughout its MTBR with the fluorophore acrylodan. The fluorescence emission of acrylodan is sensitive to the polarity of its environment: as polarity decreases, the emission maximum shifts to shorter wavelengths and the quantum yield increases.[20] Thus, acrylodan fluorescence provides residue-specific information about its local environment, which can be used to extrapolate structural features of the protein. We labeled tau with acrylodan at equivalent locations in each of the MT binding repeats, utilizing the endogenous cysteines at residues 291 (R2) and 322 (R3) and introducing cysteines at I260 (R1) and I364 (R4) (Figure 1B). In the absence of tubulin, all four constructs have comparable emission spectra, with the wavelength of maximum emission ~522 nm (SI, Figure S1). The relatively red emission wavelength and the similar peak positions across different repeats confirm that the all four labeling positions are solvent-exposed, reflecting the intrinsic disorder of tau. Upon the addition of tubulin, the fluorescence emission of each construct exhibits a significant shift to shorter wavelengths (Figure 3A) along with an increase in fluorescence intensity, indicating a less-polar environment than in solution. However, the magnitude of the shift is not the same for each construct. Specifically, the probes in R2 and R3 have a significantly larger shift (29 and 32 nm, respectively) than R1 and R4 (22 and 24 nm, respectively) (Figure 3A). These results show that the environments of probes of R2 and R3 are less polar than those of the probes of R1 and R4 when bound to tubulin. This may reflect a hierarchy in binding, whereby R2 and R3 are the primary mediators. Our findings here support previous work from our laboratory where we proposed that R3 along with one of its flanking repeat regions constitute the primary tubulin-binding domain of tau.[15]

A more detailed description of tubulin-bound tau was obtained by labeling 12 residues within the repeat sequence of R3 with acrylodan. Fluorescence emission spectra were measured in the absence and presence of tubulin. In solution, all labeling positions have comparable emission spectra with maxima at ~522 nm (SI, Figure S2). Upon binding to tubulin, the shift in emission spectra gives rise to a clear periodic pattern (Figure 3B). The magnitude of the shift varies from 24 to 48 nm, with probes closer to the N-terminus generally exhibiting larger shifts than those closer to the C-terminus. The periodicity of the signal is evocative of helical structure and

DOI: 10.1021/jacs.5b04561
J. Am. Chem. Soc. 2015, 137, 9218−9221

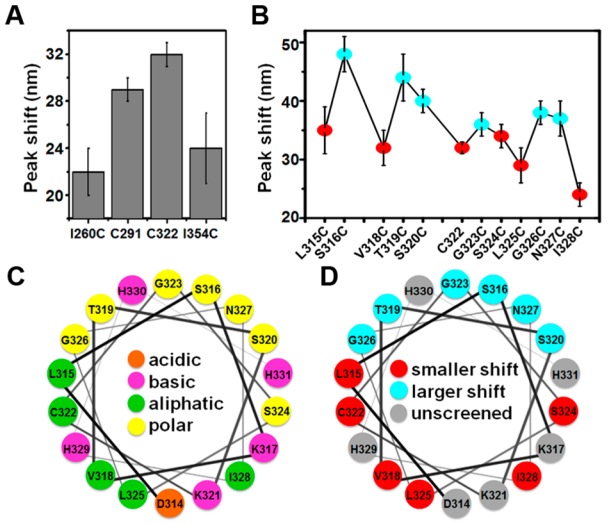

Figure 3. Acrylodan screening of tau bound to tubulin. (A) The absolute value of emission peak shifts of constructs labeled at equivalent locations in each of the four different repeat regions. (B) The absolute value of emission peak shifts of constructs throughout R3. Residues exhibiting larger than average (average = 35.6 nm) shifts are colored cyan while smaller than average shifts are colored red. (C) Helical wheel projection of R3 colored by polarity of each residue. (D) Helical wheel projection of R3 colored by the magnitude of the acrylodan fluorescence shift from B.

supports a model whereby the repeat sequences of the MTBR undergo transitions from disordered to helical upon binding to tubulin. Our observation is in excellent agreement with a recent simulation study of tau which found a high propensity for helical structure in residues 315−325 in R3.[21]

The majority of previous efforts to elucidate structural features of functional forms of tau have focused on tau in solution[22] or when bound to MTs.[14,23] Recent work from our laboratory highlights the potential importance of the interaction between tau and soluble tubulin,[15] and here we used a combination of FCS and acrylodan fluorescence to probe this interaction. Analysis of the spectral shifts of tau labeled throughout the repeat sequence of R3 with acrylodan reveal that it assumes a periodic pattern upon binding, consistent with helical structure. A projection of the sequence of R3 on a helical wheel shows that it is fairly amphipathic (Figure 3C). When the same helix is overlaid with the spectral shifts measured by acrylodan fluorescence, an intriguing pattern is revealed. The labeling positions exhibiting larger emission peak shifts overlay with the hydrophilic face of the helix, while those exhibiting smaller emission peak shifts correspond to the hydrophobic face of the helix (Figure 3C,D). The most direct interpretation of this observation is that the hydrophilic side of the R3 helix interfaces with tubulin, resulting in the less polar environment reflected in the acrylodan fluorescence at these residues. There are more charged or potentially charged residues (D314, K321, H329) on the hydrophobic side compared with the hydrophilic side (H330) of the helix. Positively charged residues have been shown to be generally important to MT binding[11b,24] and it may be that these located on the exposed hydrophobic side of the helix are important for interactions with the negatively charged C-terminal tail of tubulin.[11a] Interestingly, a similar helical structure has been observed for tau bound to anionic vesicles, although, in this study, the hydrophobic side of the helix formed the interface with the lipid bilayer.[25] Another scenario is that tau binds to tubulin through a different set of residues, triggering a conformational change in residues 315−328. Such a model is compatible with a recent NMR study which found that tau interfaces with tubulin through residues 300−317,[26] upstream of the sequence we screened. Regardless, our results reveal the importance of a disorder-to-helical transition in this region for tau binding and function.

Probing of the four repeats reveal that comparable locations in the sequence do not interact uniformly (Figure 3A). It may be that probes of R2 and R3 are more buried upon binding to tubulin than the probes of R1 and R4, or rotations of the helical regions of each repeat result in differential accessibility to solvent. It is also possible that R2 and R3 are more tightly bound to tubulin than R1 and R4, such that the probes in R1 and R4 sample both a buried, tubulin-bound conformation and a solvent-exposed, unbound conformation, which is averaged in the measured emission spectra, while R2 and R3 remain tightly associated. Interestingly, R2 and R3 shared higher sequence identity compared to R1 and R4 (SI, Figure S3) and sequences within the inter-repeats upstream of R2 and R3 have been identified as hot spots for tau-MT interactions.[14a] Our results suggest that the intrinsic differences existing between each repeat may be crucial to the function of tau as a MT-polymerization promoter.

The differential signal arising from the different repeats may also reflect binding to different tubulin dimers. Our FCS measurements, corroborated by chemical cross-linking (SI, Figure S4), support a model whereby tau binds to multiple tubulin dimers, at least in the presence of excess tubulin. While we are not able to determine an exact stoichiometry, it has been reported previously that tau can form complexes with tubulin dimers at 1:2 or 1:4 ratios, with subsequent self-assembly into ring structures.[27] These experiments were carried out at much higher tau concentrations and larger tau: tubulin ratios. However, they are largely consistent with our observations at the single-molecule level, supporting the idea that tau's ability to associate with multiple tubulin subunits may be important to its function. Strikingly, we observe this even when the polymerization-inhibiting constructs DARPin and RB3 are present (Figure 2B).

We can consider a model of the tau-tubulin complex in light of what we know about the DARPin-tubulin and RB3-tubulin complexes. DARPin caps the β-subunit and blocks longitudinal interaction between dimers.[17] Tau may therefore laterally cross-link DARPin-tubulin complexes to form the larger assemblies we observe. RB3-tubulin includes a longitudinal interaction between tubulin dimers.[18] The similar size of the tau-RB3-tubulin and tau-tubulin complexes indicates that tau is able to mediate these longitudinal tubulin interactions as well (Figure 4). This is in agreement with a recent NMR study which demonstrated longitudinal assembly of tubulin dimers by a tau fragment.[28] Overall, our results suggest that tau can mediate both lateral and longitudinal interactions between tubulin dimers, or potentially between soluble tubulin and the MT lattice. The intrinsic disorder of tau may provide the flexibility needed to mediate these variable types of association.

In this work we provide structural insight into tau-tubulin assemblies using a combination of FCS and acrylodan fluorescence screening. Our results provide evidence of helical structure in the MTBR of tau bound to its functional partner, tubulin. Moreover, they demonstrate simultaneous association with multiple tubulin dimers, providing insight into a potential mechanism for tau-mediated polymerization of tubulin.

DOI: 10.1021/jacs.5b04561
J. Am. Chem. Soc. 2015, 137, 9218−9221

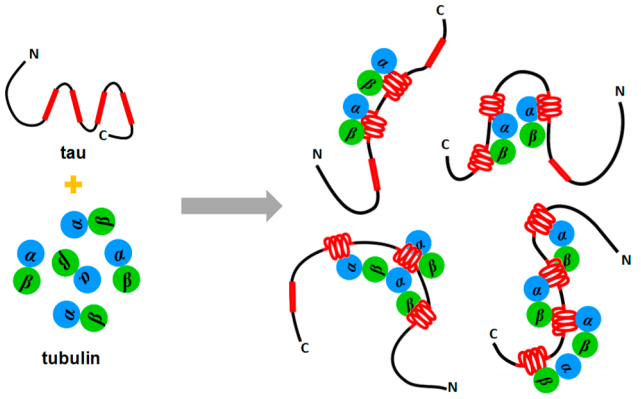

Figure 4. Cartoon illustrating tau-tubulin complexes formed under non-assembly conditions. Upon binding to tubulin, regions of the MTBR become helical. Tau's flexible, dynamic structure mediates binding to multiple tubulin dimers through its inter-repeat/repeat sequences.

■ ASSOCIATED CONTENT

Supporting Information

Experimental methods, models produced by protein docking, corrections to diffusion time calculations, sequence alignments, and other controls. The Supporting Information is available free of charge on the ACS Publications website at DOI: 10.1021/jacs.5b04561.

■ AUTHOR INFORMATION

Corresponding Author

*elizabeth.rhoades@sas.upenn.edu

Present Address

[‖]Department of Chemistry, University of Pennsylvania, Philadelphia, Pennsylvania 19104, United States.

Notes

The authors declare no competing financial interest.

■ ACKNOWLEDGMENTS

The authors thank L. A. Metskas for help creating tau models, M. Birol for help with protein docking, and L. Binder, L. Regan, and M. Knossow for tau, pET-HT, and DARPin plasmids, respectively. The authors acknowledge the Yale Chemical and Biophysical Instrumentation Center for use of their lifetime fluorimeter. This work was supported by NSF MCB 0919853 (to E.R.) and by NSF DBI 1156585 and the Raymond and Beverly Sackler Institute for Biological, Physical, and Engineering Sciences (to J.A.C.).

■ REFERENCES

(1) (a) Weingarten, M. D.; Lockwood, A. H.; Hwo, S. Y.; Kirschner, M. W. *Proc. Natl. Acad. Sci. U. S. A.* **1975**, *72*, 1858−1862. (b) Drubin, D. G.; Kirschner, M. W. *J. Cell Biol.* **1986**, *103*, 2739−2746.

(2) Mandelkow, E. M. *Trends Cell Biol.* **1998**, *8*, 425−427.

(3) Harada, A.; Oguchi, K.; Okabe, S.; Kuno, J.; Terada, S.; Ohshima, T.; Satoyoshitake, R.; Takei, Y.; Noda, T.; Hirokawa, N. *Nature* **1994**, *369*, 488−491.

(4) Ballatore, C.; Lee, V. M. Y.; Trojanowski, J. Q. *Nat. Rev. Neurosci.* **2007**, *8*, 663−672.

(5) (a) Vershinin, M.; Carter, B. C.; Razafsky, D. S.; King, S. J.; Gross, S. P. *Proc. Natl. Acad. Sci. U. S. A.* **2007**, *104*, 87−92. (b) Dixit, R.; Ross, J. L.; Goldman, Y. E.; Holzbaur, E. L. F. *Science* **2008**, *319*, 1086−1089.

(6) Mazanetz, M. P.; Fischer, P. M. *Nat. Rev. Drug Discovery* **2007**, *6*, 464−479.

(7) Butner, K. A.; Kirschner, M. W. *J. Cell Biol.* **1991**, *115*, 717−730.

(8) Gustke, N.; Trinczek, B.; Biernat, J.; Mandelkow, E. M.; Mandelkow, E. *Biochemistry* **1994**, *33*, 9511−9522.

(9) Chen, J.; Kanai, Y.; Cowan, N. J.; Hirokawa, N. *Nature* **1992**, *360*, 674−676.

(10) Brandt, R.; Leger, J.; Lee, G. *J. Cell Biol.* **1995**, *131*, 1327−1340.

(11) (a) Chau, M. F.; Radeke, M. J.; de Ines, C.; Barasoain, I.; Kohlstaedt, L. A.; Feinstein, S. C. *Biochemistry* **1998**, *37*, 17692−17703. (b) Goode, B. L.; Chau, M.; Denis, P. E.; Feinstein, S. C. *J. Biol. Chem.* **2000**, *275*, 38182−38189.

(12) Goode, B. L.; Denis, P. E.; Panda, D.; Radeke, M. J.; Miller, H. P.; Wilson, L.; Feinstein, S. C. *Mol. Biol. Cell* **1997**, *8*, 353−365.

(13) Al-Bassam, J.; Ozer, R. S.; Safer, D.; Halpain, S.; Milligan, R. A. *J. Cell Biol.* **2002**, *157*, 1187−1196.

(14) (a) Mukrasch, M. D.; Biernat, J.; von Bergen, M.; Griesinger, C.; Mandelkow, E.; Zweckstetter, M. *J. Biol. Chem.* **2005**, *280*, 24978−24986. (b) Eliezer, D.; Barre, P.; Kobaslija, M.; Chan, D.; Li, X. H.; Heend, L. *Biochemistry* **2005**, *44*, 1026−1036.

(15) Elbaum-Garfinkle, S.; Cobb, G.; Compton, J. T.; Li, X. H.; Rhoades, E. *Proc. Natl. Acad. Sci. U. S. A.* **2014**, *111*, 6311−6316.

(16) Magde, D.; Webb, W. W.; Elson, E. *Phys. Rev. Lett.* **1972**, *29*, 705−708.

(17) Pecqueur, L.; Duellberg, C.; Dreier, B.; Jiang, Q. Y.; Wang, C. G.; Pluckthun, A.; Surrey, T.; Gigant, B.; Knossow, M. *Proc. Natl. Acad. Sci. U. S. A.* **2012**, *109*, 12011−12016.

(18) (a) Gigant, B.; Curmi, P. A.; Martin-Barbey, C.; Charbaut, E.; Lachkar, S.; Lebeau, L.; Siavoshian, S.; Sobel, A.; Knossow, M. *Cell* **2000**, *102*, 809−816. (b) Barbier, P.; Dorleans, A.; Devred, F.; Sanz, L.; Allegro, D.; Alfonso, C.; Knossow, M.; Peyrot, V.; Andreu, J. M. *J. Biol. Chem.* **2010**, *285*, 31672−31681.

(19) Pierce, B. G.; Wiehe, K.; Hwang, H.; Kim, B. H.; Vreven, T.; Weng, Z. P. *Bioinformatics* **2014**, *30*, 1771−1773.

(20) Prendergast, F. G.; Meyer, M.; Carlson, G. L.; Iida, S.; Potter, J. D. *J. Biol. Chem.* **1983**, *258*, 7541−7544.

(21) Luo, Y.; Ma, B. Y.; Nussinov, R.; Wei, G. H. *J. Phys. Chem. Lett.* **2014**, *5*, 3026−3031.

(22) (a) Mukrasch, M. D.; Bibow, S.; Korukottu, J.; Jeganathan, S.; Biernat, J.; Griesinger, C.; Mandelkow, E.; Zweckstetter, M. *PLoS Biol.* **2009**, *7*, 399−414. (b) Harbison, N. W.; Bhattacharya, S.; Eliezer, D. *PLoS One* **2012**, *7*, e34679. (c) Narayanan, R. L.; Durr, U. H. N.; Bibow, S.; Biernat, J.; Mandelkow, E.; Zweckstetter, M. *J. Am. Chem. Soc.* **2010**, *132*, 11906−11907.

(23) Mukrasch, M. D.; von Bergen, M.; Biernat, J.; Fischer, D.; Griesinger, C.; Mandelkow, E.; Zweckstetter, M. *J. Biol. Chem.* **2007**, *282*, 12230−12239.

(24) Goode, B. L.; Feinstein, S. C. *J. Cell Biol.* **1994**, *124*, 769−782.

(25) Georgieva, E. R.; Xiao, S.; Borbat, P. P.; Freed, J. H.; Eliezer, D. *Biophys. J.* **2014**, *107*, 1441−1452.

(26) Kadavath, H.; Hofele, R. V.; Biernat, J.; Kumar, S.; Tepper, K.; Urlaub, H.; Mandelkow, E.; Zweckstetter, M. *Proc. Natl. Acad. Sci. U. S. A.* **2015**, *112*, 7501−7506.

(27) Devred, F.; Barbier, P.; Douillard, S.; Monasterio, O.; Andreu, J. M.; Peyrot, V. *Biochemistry* **2004**, *43*, 10520−10531.

(28) Gigant, B.; Landrieu, I.; Fauquant, C.; Barbier, P.; Huvent, I.; Wieruszeski, J. M.; Knossow, M.; Lippens, G. *J. Am. Chem. Soc.* **2014**, *136*, 12615−12623.

DOI: 10.1021/jacs.5b04561
J. Am. Chem. Soc. 2015, 137, 9218−9221